

Manganese mobilization from the Western Continental margin of India

D. N. Yadav

Physical Research Laboratory, Ahmedabad 380 009, India

The Western Continental margin of India (WCMI) exhibits distinct features with respect to vertical distribution of manganese in sediments. There is no significant manganese downcore variation in upper slope sediments whereas high concentration (by an order of magnitude relative to bottom sections) has been observed in top sediment cores for the lower slope region. Also, in the upper slope sediments, average manganese concentration is low by a factor of three compared to that (~1000 ppm) transported by the Narmada/Tapti river suspended particles. The low manganese concentration is attributed to its reductive mobilization. Typical value of manganese flux being mobilized into overlying seawater from reducing upper slope sediments covering an area of 5°Lat × 3°Long is calculated to be 3×10^{10} g/y, which is nearly 10% of dissolved manganese supply to the ocean by world rivers. Although calculated flux of manganese mobilized from upper slope sediments is not the highest among the values from other margin regions, yet this shows a potential source for dissolved manganese in seawater. Interestingly, the calculated carbon oxidation flux (based on manganese reduction rate) in the upper slope sediments is found to be less than 1% of primary productivity and, thus it provides a limiting value of organic matter combustion. Contrary to upper slope sediments, there is no significant supply of soluble manganese to overlying seawater, which is expected due to prevailing oxidizing conditions at the sediment-water interface in the lower slope region.

THE biogeochemical cycle of Mn in marine environment plays an important role in regulating trace metal distribution, as manganese oxides are potential scavengers of several trace metals¹. In sediments, Mn oxides undergo reduction to soluble Mn²⁺ during anaerobic decomposition of organic matter^{2,3}.



Therefore, in reducing conditions Mn is released from sediments to pore waters and is subsequently transported to overlying seawater by advective-diffusion processes either in part or completely depending on the redox conditions near the sediment-water interface. In this mobilization process, only some fraction of Mn (reactive component) associated with continental/riverine sediment

inputs is mobilized, leaving behind some fraction in the sediments. At some places of margin regions⁴, high concentration of Mn is reported in top oxidizing sedimentary layer as it acts as a cap for Mn²⁺ escape from below the sediments. These are the major pathways of Mn cycling in margin regions. Release of Mn²⁺ from reducing sediments and thereafter supply to overlying seawater generally takes place if manganese oxidation rate at sediment-water interface is slower than that of its reduction rate in the sediment below the surface⁵⁻⁷. Factors controlling release of Mn²⁺ from sediments to overlying seawater and its distribution in various layers within the sediments include not only the bottom water O₂ concentration⁸⁻⁹, temperature and organic input^{3,7} but also depend on precipitation of authigenic carbonate mineral phases such as calcite¹⁰⁻¹² and Mn-carbonate¹³⁻¹⁴ from the pore waters. Carbonate mineral phases in the sediment can act as a sink for soluble Mn²⁺. Also, sediments characterized by bioturbation show increased supply rate of Mn²⁺ to the overlying seawater^{5-9,15}.

Earlier studies in sediments from the Western Continental margins of India (WCMI) have shown depletion of Mn along the open shelf and slope regions^{16,17}. More recently, Somayajulu *et al.*¹⁸ attributed variations in the concentrations of manganese in sediments from the shelf and slope regions of WCMI to be due to differences in prevailing redox conditions. This paper synthesizes available data on the manganese distribution in WCMI sediments to obtain constraints on its fluxes to the overlying water column and its role in mineralization of organic matter.

Materials and methods

Five spade sediment cores (50 × 30 × 20 cm) from the WCMI region (Figure 1) were collected during December 1988. Of these, three cores (L-8, J-7 and I-5) are from the upper slope region (water depth ranging from 280 to 350 m) where the core of denitrification layer (centered at ~300 m depth)¹⁹ meets the sediment-water interface. The remaining two cores, viz. K-11 and M-12 are from the lower slope region where water depth is ~2500 m. Immediately after collection, sub-cores of ~5 cm diameter and ~30 cm in length were taken from these spade cores. The sub-cores were sampled at 1–2 cm

depth intervals for CaCO_3 , loss on ignition (LOI), major, trace elements and radionuclide measurements. Intense H_2S smell was felt during sectioning of the cores L-8 and J-7 at about ~5 cm below the surface, indicating strong anoxic conditions prevailing near the surface of these cores. On the contrary, no H_2S smell was felt from any layer while sectioning the cores from the lower slope region. Chronology of these cores was determined mainly by the $^{210}\text{Pb}_{\text{excess}}$ and ^{137}Cs methods^{17,18}.

Results and discussion

It is well documented that in anoxic marine sediments, where sediment accumulation is relatively high, manganese is mobilized as Mn(II) from the solid phase to solution²⁰⁻²². In margin areas, the primary source of Mn to sediments is land-derived. Hence, one of the approaches to obtain information on Mn mobilization is to compare the abundance of Mn in margin sediments with that in fluvial sediments. Such study has an important implication to elucidate high content of manganese in deep ocean sediments. In fact, early sediment diagenesis leading to recycling of manganese from near-shore region is considered to be an important 'source' for high manganese concentration in deep ocean reservoir. For instance, suggestion has been made by several workers that a 'source' of Mn to the central North Pacific may be from reduced continental shelf sediments²³⁻²⁷. In the following, manganese mobilization that occurs across the transect encompassing both anoxic (upper slope) and oxic (lower slope) sedimentary environments of the Arabian sea are discussed.

Upper slope sediments (L-8, J-7 and I-5)

The depth profiles of manganese in these sediments are

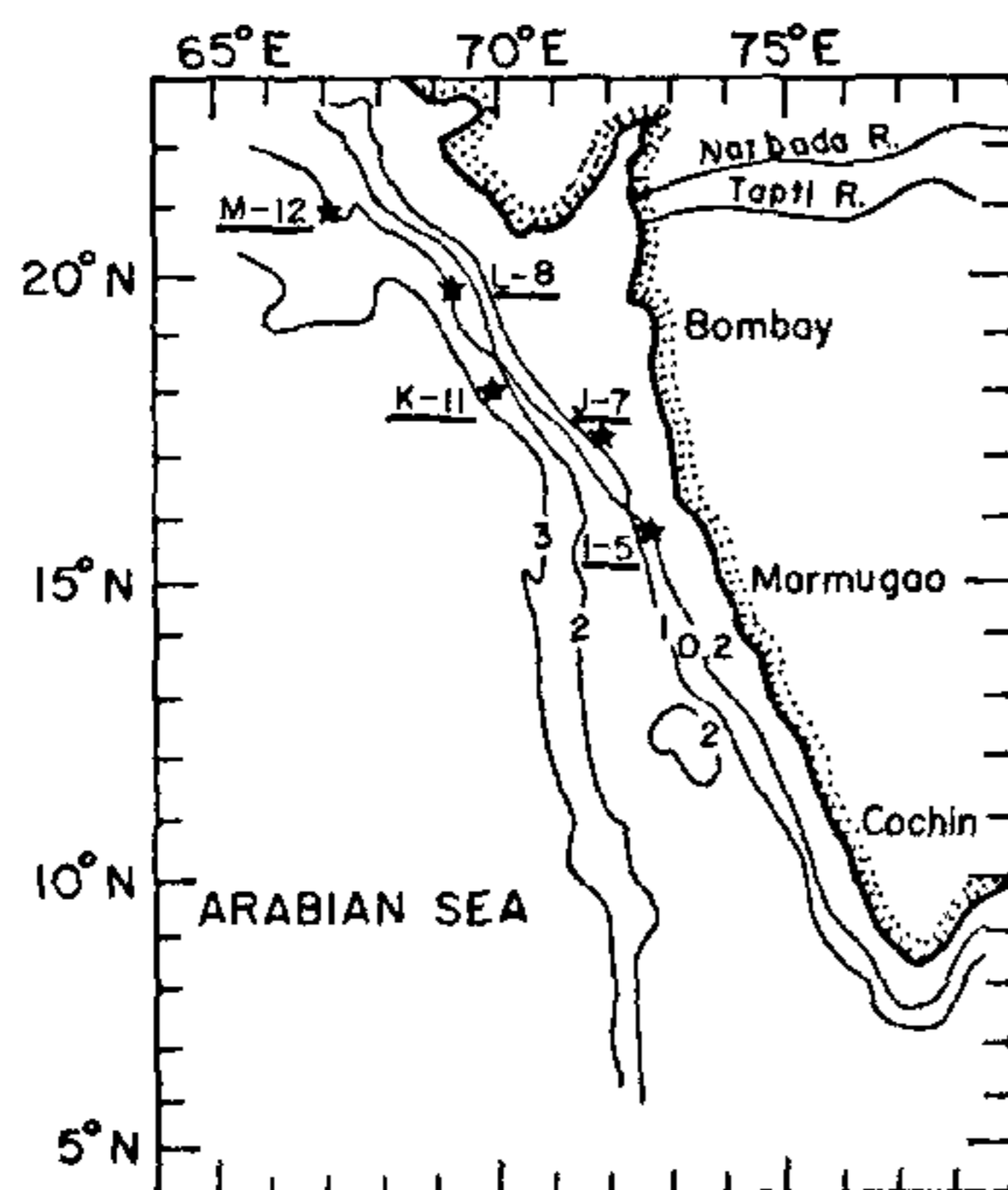


Figure 1. Map showing core locations (*) along the WCMI with water-depth contours in km.

presented in Table 1 and Figure 2a, though they have been published earlier^{17,18}. The manganese concentration in all these cores is generally low (~285–350 ppm, Table 1a) compared to that in the Narmada and Tapi river suspended particles (~1000 ppm)¹⁶. The low Mn concentration in these sediment cores relative to the source material is attributed to the reductive mobilization of Mn from the sedimentary column. As the upper slope sediments are from shallow water depths, manganese mobilization from fluvial sediments and particulates during their transit through anoxic denitrification water layer is expected to be minimal. With this assumption, a simple calculation is done to estimate the flux of Mn being mobilized from the upper slope reducing sediments.

The flux of manganese mobilized from sedimentary column, F_{Mn} ($\mu\text{g}/\text{cm}^2 \cdot \text{y}$), can be obtained using the relation

$$F_{\text{Mn}} = S \cdot \rho (C_r - C_s), \quad (2)$$

where S is the sediment accumulation rate (cm/y), ρ the in-situ density (g/cm^3) of the sediment, C_r and C_s are the manganese concentrations in river particles (~1000 ppm)¹⁶ and in upper slope sediments. The value of F_{Mn} for the three cores L-8, J-7 and I-5 is calculated to be 7.4, 68.7 and 17 $\mu\text{g}/\text{cm}^2 \cdot \text{y}$ respectively using their column average Mn concentration (Table 1a), density (0.44, 0.58 and 0.61 g/cm^3) (refs 28, 29) and rate of sediment accumulation (0.025, 0.183 and 0.039 cm/y)^{18,28}. In this method of flux calculation for manganese, there is some degree of uncertainty associated with the assumption of constant Mn concentration (~1000 ppm) in river-borne suspended sediments. Earlier study has shown that Narmada and Tapi rivers which drain into the study region show a slight seasonal variation in manganese concentration of suspended particles (Narmada: 1000–

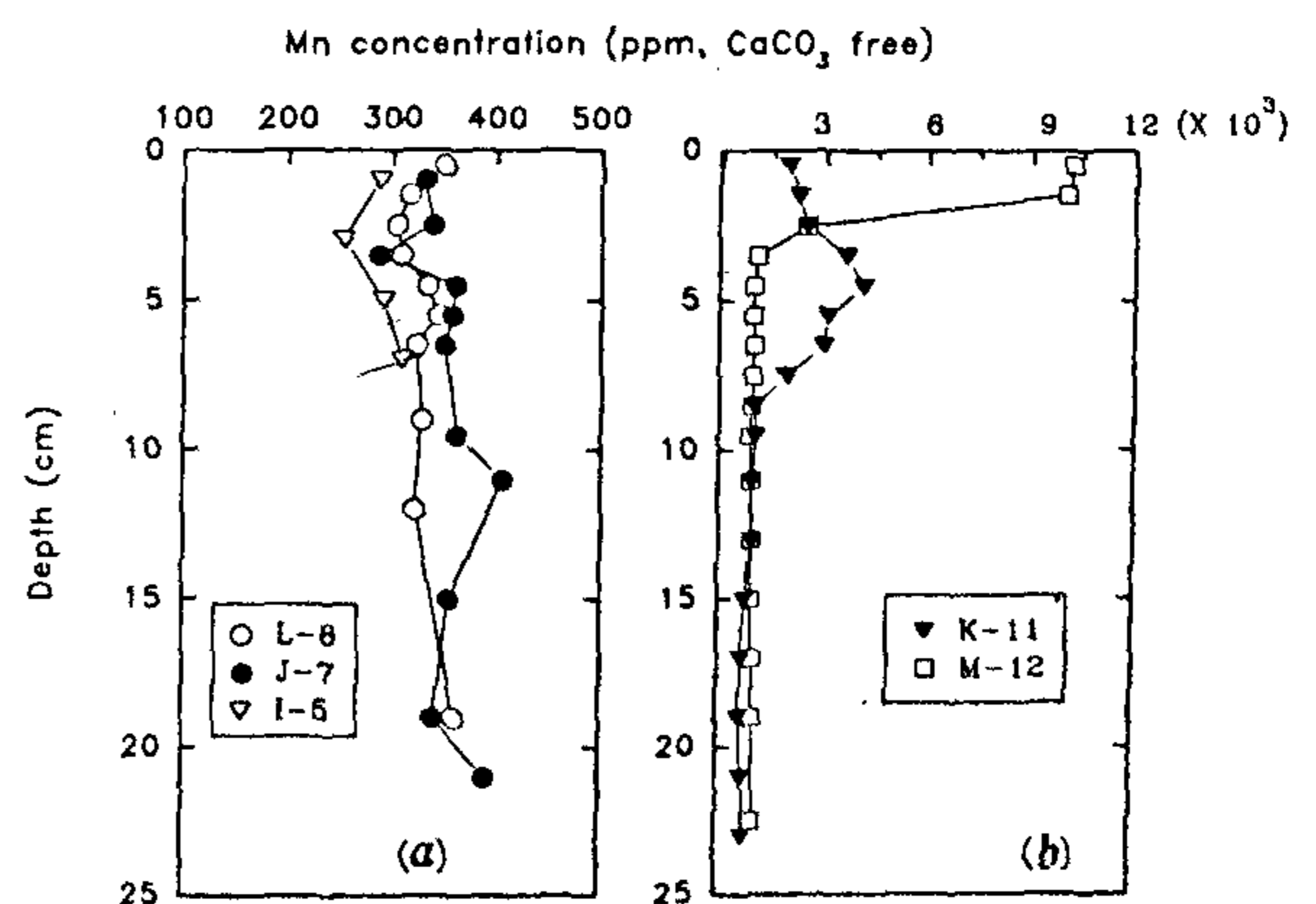


Figure 2. Downcore variation of Mn abundance in the lower slope sediments. The Mn distribution in the lower slope sediments shows a distinct structure with high values near the sediment-water interface.

Table 1a. Mn concentration in the upper slope sediments on CaCO₃ free basis

Core: L-8		Core: J-7		Core: I-5	
Depth (cm)	Mn (ppm)	Depth (cm)	Mn (ppm)	Depth (cm)	Mn (ppm)
(0-1)	349	(0-2)	330	(0-2)	287
(1-2)	316	(2-3)	339	(2-4)	253
(2-3)	303	(3-4)	286	(4-6)	291
(3-4)	308	(4-5)	360	(4-6) <i>R</i>	273
(3-4) <i>R</i>	314	(5-6)	357	(6-8)	310
(4-5)	333	(6-7)	349		
(5-6)	343	(9-10)	362		
(6-7)	323	(10-12)	406		
(8-10)	328	(14-16)	354		
(10-14)	321	(18-20)	340		
(18-20)	359	(20-22)	390		
$\overline{\text{Mn}} =$	327*	$\overline{\text{Mn}} =$	352*	$\overline{\text{Mn}} =$	283*

*Concentration averaged over entire core length.
R denotes replicate analysis.

Table 1b. Mn concentration in the lower slope sediments on CaCO₃ free basis

Core: K-11		Core: M-12	
Depth (cm)	Mn (ppm)	Depth (cm)	Mn (ppm)
(0-1)	1903	(0-1)	10161
(1-2)	2211	(1-2)	10017
(2-3)	2479	(2-3)	2470
(3-4)	3581	(3-4)	997
(4-5)	4092	(4-5)	908
(5-6)	3052	(4-5) <i>R</i>	930
(6-7)	2952	(5-6)	897
(7-8)	1862	(6-7)	947
(7-8) <i>R</i>	1841	(7-8)	889
(8-9)	922	(8-9)	847
(9-10)	975	(9-10)	810
(10-12)	881	(10-12)	865
(12-14)	865	(12-14)	864
(12-14) <i>R</i>	839	(14-16)	884
(14-16)	692	(16-18)	887
(16-18)	574	(18-20)	944
(18-20)	564	(20-25)	958
(20-22)	631		
(22-24)	711		
$\overline{\text{Mn}}^*$	1340	$\overline{\text{Mn}}^*$	1270

* $\overline{\text{Mn}}$ indicates median value of concentration over entire core length.
R denotes replicate analysis.

1300 ppm, Tapti: 1200-1300 ppm)¹⁶. With this uncertainty, a typical value of manganese flux from upper slope reducing sediments to overlying seawater can be taken as 21 $\mu\text{g}/\text{cm}^2 \cdot \text{y}$, which is the geometric mean of Mn fluxes for three cores. If this calculation is extended to an area of 5°Lat. \times 3°Long., bounded by these cores, the flux of Mn would be $\sim 3.0 \times 10^{10}$ g/y which is nearly

10% of the dissolved Mn ($\sim 3 \times 10^{11}$ g/y) transported by world rivers to ocean²⁷. Such a high flux of Mn out of sediments from the upper slope region of the Arabian Sea emphasizes the importance of mobilization of Mn in the margin region. It is likely that manganese released from these sediments is a source of dissolved Mn maxima reported in the Arabian Sea intermediate waters³⁰⁻³¹. In order to evaluate the importance of manganese mobilization from reducing sediments as 'source' for seawater, benthic chamber study is necessitated³².

Table 2 compares the flux of Mn released from river-borne particles from the upper slope sediments of the Arabian Sea with the fluxes reported from other coastal margin areas of the world ocean. The flux of Mn solubilized is generally related to rates of sedimentation, biological productivity and also to the particle mixing by bioturbation⁴. Sundby and Silverberg³³ have studied manganese cycling in Laurentian trough (water depth, 300-400 m) and applied a diagenetic model and mass-balance calculations to derive the Mn flux. They observed a net flux of 140-180 $\mu\text{g}/\text{cm}^2 \cdot \text{y}$ (Table 2). The magnitude of particle mixing by bioturbation considerably influences the rate of Mn cycling both in the sediment core (internal cycling) and the fraction mobilizing to overlying seawater. Trefry and Presley³⁴ have interpreted the deficiency of Mn in the Mississippi delta sediments, compared to that in the river particulates, as due to its mobilization under reducing conditions. Using the concentration gradient of Mn in sediment pore waters, they calculated the outgoing diffusive manganese flux from sediments (water depth < 100 m) in the range of 30-850 $\mu\text{g}/\text{cm}^2 \cdot \text{y}$ (Table 2). Johnson *et al.*³² have

Table 2. The benthic manganese flux from margin sediments

Margin sites	Mn flux ($\mu\text{g}/\text{cm}^2 \cdot \text{y}$)	Reference
WCMI (upper slope)	~ 35	This study,
Central California coast line	~ 10	Johnson <i>et al.</i> ¹⁴
Gulf of St. Lawrence	~ 140–180	Sundby and Silverberg ³³
Mississippi Delta	~ 30–850	Trefry and Presley ³⁴
Eastern Bering shelf	~ 1	Heggie <i>et al.</i>

reported an average benthic Mn flux of $\sim 10 \mu\text{g}/\text{cm}^2 \cdot \text{y}$ from the central California continental margin.

In the present study, the estimated high flux of manganese, $21 \mu\text{g}/\text{cm}^2 \cdot \text{y}$ from the upper slope region of WCMI (Table 2), points out the importance of WCMI in controlling the overall marine budget of manganese in seawater. In this regard, more rigorous and quantitative information on manganese flux calculation is necessitated by studying concentration gradient of manganese in sediment pore waters.

Lower slope sediments (K-11 and M-12)

The manganese distribution in the two cores, K-11 and M-12, from the lower slope region shows features, which are distinctly different from those observed in the upper slope sediment cores. These two cores have high Mn concentrations (~ 1900 and 10160 ppm on CaCO_3 free basis) occurring in surface sections (Figure 2b, Table 1b)^{18,28}. In core M-12 the Mn concentration decreases with depth and attains a value of 900 ppm, for K-11 the Mn concentration shows a shallow depth (4–5 cm) maximum and then decreases to a value of ~ 700 ppm below 10 cm depth. Such a distribution of Mn is typical of the slope sediments where Mn released at depths in the sedimentary column by diagenetic processes is sequestered at the oxic sediment–water interface^{15,33,35}. In contrast to the average value of Mn for upper slope sediments, the median value (Median of Mn concentration has been taken owing to large downcore variations in manganese data, see Figure 2b) of Mn concentration (on a CaCO_3 free basis) taken over the entire core length for K-11 and M-12, is ~ 1340 and ~ 1270 ppm respectively. These values of Mn are comparable with that of fluvial sediments transported by the Narmada/Tapti rivers¹⁶. These data suggest that there is no net mobilization of Mn, but only its redistribution within the column.

A model calculation has been done to determine manganese reduction rate, which in turn provides carbon oxidation flux for the lower slope sediments in the column itself. For this, out of the two cores, only M-12 could be modelled using the concept of Aller^{5,15}, because required exponential function for manganese distribution could be fitted with this core. In the following, discussion

is made on application of Aller model^{5,15} to elucidate oxidation of C_{org} based on Mn distribution in the core M-12.

In the lower slope sediments, the depth profile of 'excess' Mn concentration can be represented by particle mixing and Mn reduction rate as proposed by Aller⁵. This is represented by

$$\frac{\partial C_s}{\partial t} = D \cdot \frac{\partial^2 C_s}{\partial z^2} - R = 0, \quad (3)$$

where D is the mixing coefficient, C_s is the solid-phase 'excess' Mn concentration and R is the Mn reduction rate. For shorter core length, say about 5 cm, D is generally assumed to be constant^{5,15}. Also, an assumption is made that manganese mobilized by reduction–oxidation process is internal, and there is no leakage of Mn^{2+} to the overlying water. The 'excess' manganese [i.e. total solid-phase Mn minus the average background (background Mn concentration refers to unreactive Mn which remains almost constant after a certain depth from the surface) value in $\mu\text{g}/\text{g}$] in top (0–4 cm) of the core M-12 is converted in units of mass/volume ($\mu\text{M}/\text{cm}^3$) by using *in-situ* sediment density of $0.33 \text{ g}/\text{cm}^3$ and its depth profile is fitted with an exponential function⁴:

$$C_s = C_0 \cdot e^{-\beta \cdot z}, \quad (4)$$

where C_s and C_0 are the solid phase Mn concentration at any depth and at the sediment surface respectively and β is the attenuation coefficient. Attenuation constant

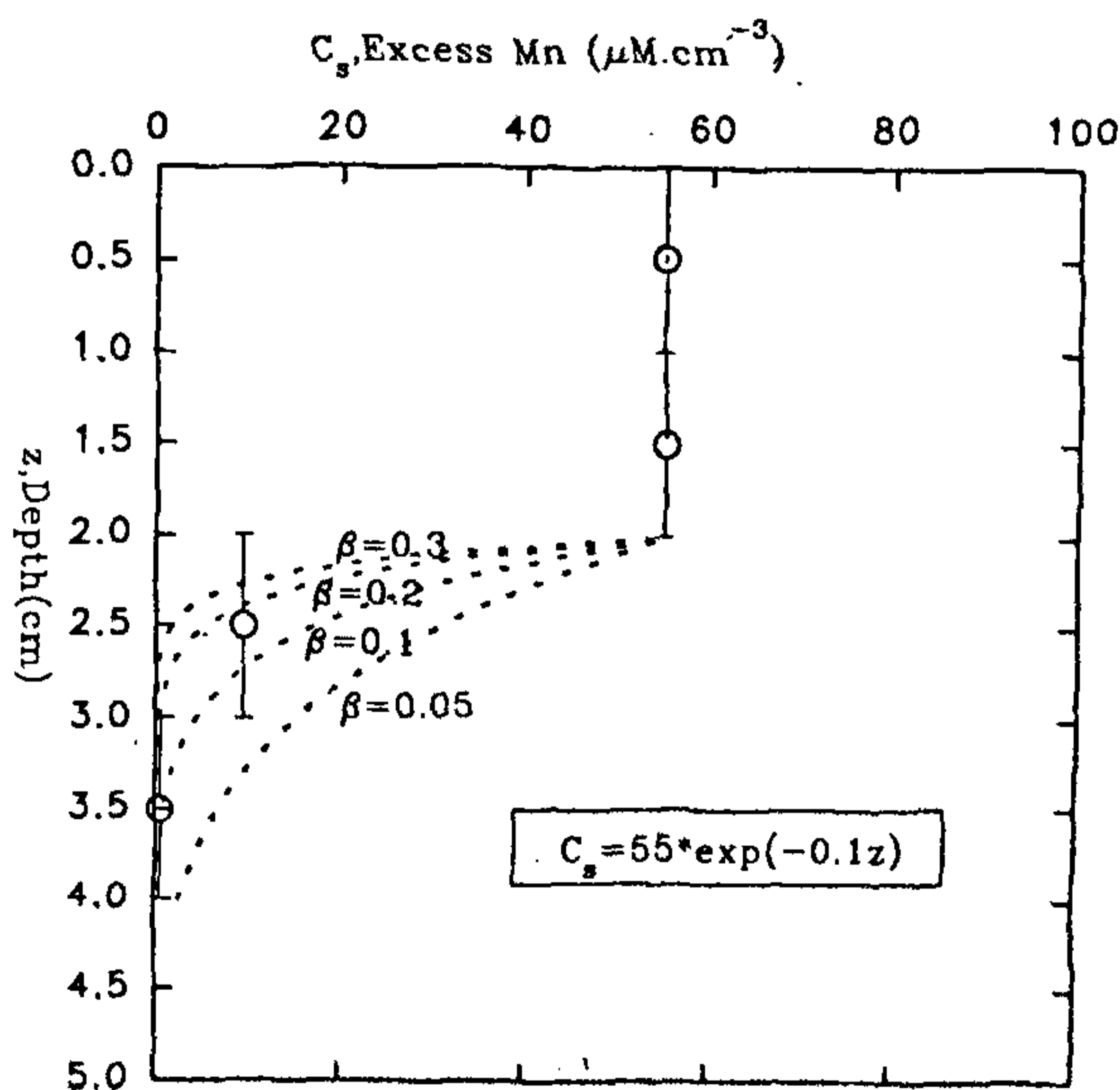


Figure 3. Experimental data for the sediment core M-12 fitted with the exponential function for different values of β (see text for explanation).

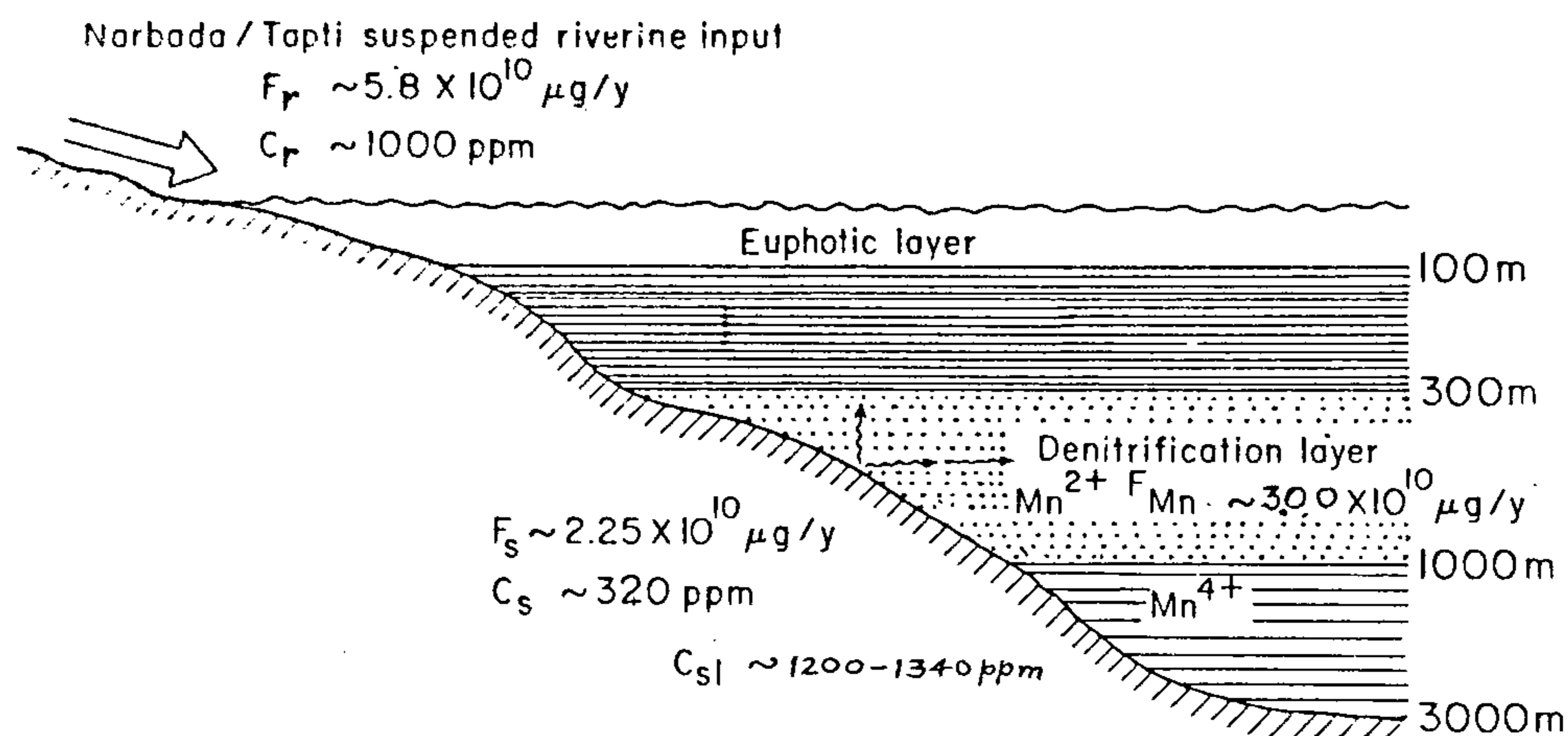
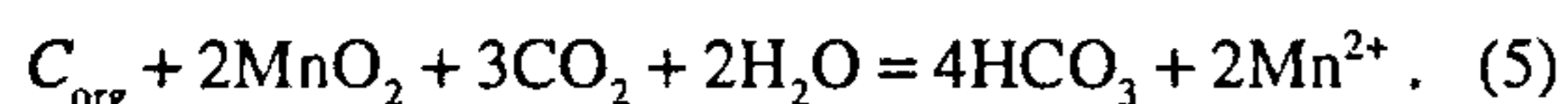


Figure 4. Schematic diagram showing Mn cycling between sediment and seawater along the WCMI region that represents $5^\circ\text{Lat.} \times 3^\circ\text{Long.}$ area. C_r is concentration and F_r the flux of Mn transported by riverine suspended matters. C_s and F_s refer to concentration and flux of Mn mobilized from reducing upper slope sediments to the denitrification layer. C_{sl} is the average concentration of Mn in lower slope sediments. Although dissolved riverine Mn input and atmospheric transport are neglected, a reasonable degree of balance is observed between F_r and $(F_s + F_{Mn})$.

(β) controls decay profile of 'excess' manganese concentration with depth which is dependent on particle mixing and bioturbation. The best fit with experimental data by the exponential function (with varying β) is shown in Figure 3. It is clear from the figure that the most suitable β value for Mn distribution in the core is 0.1 cm^{-1} . The only unknown in eqn (3) is D for determining (R), the Mn reduction rate. Assuming that the exponential depth profile of $^{210}\text{Pb}_{\text{excess}}$ in top 10 cm of M-12 is solely due to particle mixing (assumption seems to be reasonable since bioturbation is important for lower slope sediments owing to prevalence of oxic conditions at the sediment-water interface), the mixing coefficient D (ref. 36) is calculated to be $0.18 \text{ cm}^2/\text{y}$ which is an upper limit for particle mixing in the core M-12. This value of mixing coefficient is within the range ($0.04\text{--}0.4 \text{ cm}^2 \cdot \text{y}^{-1}$) (ref. 37) often cited for deep sea sediments.

Using this value of D and exponential function for 'excess' Mn concentration in eqn (4) which results R , the Mn reduction rate, integral of R over the depth interval for which 'excess' Mn is observed, yields an average Mn reduction flux of $0.33 \mu\text{M}/\text{cm}^2 \cdot \text{y}$. This information on Mn reduction flux is related to C_{org} oxidation flux within the sedimentary column, the details of which are given below.

The manganese reduction in nearshore sediments is represented by the following relation⁹



This shows that two moles of Mn^{2+} are generated during the oxidation of one mole of C_{org} . Therefore, it

is possible to estimate the amount of C_{org} oxidized from the Mn^{2+} released based on this stoichiometry. Such an estimate in the present study would be an upper limit for the amount of organic carbon mineralized because of two reasons: (i) uptake of Mn^{2+} by manganese carbonate precipitation in sediments from pore waters^{13,14} is neglected, and (ii) reduction of Mn oxides by abiotic/inorganic reactions³⁸ is ignored.

Considering manganese reduction flux of $0.33 \mu\text{M}/\text{cm}^2 \cdot \text{y}$ and following eqn (5), the flux of organic carbon oxidized in lower slope sedimentary column is $\sim 0.16 \mu\text{M}/\text{cm}^2 \cdot \text{y}$. Similarly, based on estimate of Mn flux (range, $7\text{--}69 \mu\text{g}/\text{cm}^2 \cdot \text{y} \equiv 0.1\text{--}1.0 \mu\text{M}/\text{cm}^2 \cdot \text{y}$) mobilized from the upper slope, the oxidation rate of C_{org} is calculated to be in the range of 0.05 to $0.5 \mu\text{M}/\text{cm}^2 \cdot \text{y}$. Comparing this flux with the primary production ($\sim 1500 \mu\text{M C}/\text{cm}^2 \cdot \text{y}$) as reported for upper slope region³⁹, it implies that the reduction of Mn contributes to $<1\%$ oxidation of C_{org} fixed by the photosynthetic activity. This indicates that C_{org} oxidation up to a stage of Mn reduction in sediments from the upper slope region may be a lower limit for organic matter combustion. More extensive study of this kind is required over the Arabian Sea region to establish relationship between manganese reduction rate and the carbon oxidation flux at the sediment-water interface. The results obtained from this study have direct relevance to the objectives of the ongoing JGOFS (India) programme.

The manganese cycling between solid and aqueous phases along the WCMI has been shown in Figure 4. A reasonable degree of balance is observed between the flux of manganese transported through Norbada/Tapti riverine sediments ($F_r \sim 5.8 \times 10^{10} \mu\text{g}/\text{y}$) and the sum of

fluxes that mobilized into seawater and the net burial rate of Mn ($F_S + F_{Mn} \sim 5.3 \times 10^{10} \mu\text{g/y}$) in the upper slope sediments. F_S , the net burial flux of manganese is calculated by assuming typical concentration of ~ 300 ppm, density of 0.5 g/cm^3 and rate of sediment accumulation 1 mm/y for the upper slope region. Furthermore, an assumption is made that contribution of Mn from its dissolved component through rivers and atmospheric transport is negligible. Figure 4 shows that the median value of Mn over the core length for the lower slope sediments is comparable with that of river suspended particles and average crustal rock composition. Thus, isopycnal transport of soluble manganese from upper slope sediments to oxidizing lower slope sediments, as is expected, is not a significant phenomenon. In the lower slope sediments, therefore, most likely the manganese cycling is internal in nature and its depth profile is controlled by microbial diagenetic processes.

1. Turekian, K. K., *Geochim. Cosmochim. Acta*, 1977, **41**, 1139–1144.
2. Froelich, P. N., Klinkhammer, G. P., Bender, M. L., Luedke, N. A., Heath, G. R., Cullend, Dauphin, P., Hammond, D., Hartman, B. and Maynard, V., *Geochim. Cosmochim. Acta*, 1979, **43**, 1075–1090.
3. Hunt, C. D. and Kelly, J. R., *Estuarine Coast. Shelf Sci.*, 1988, **26**, 527–558.
4. Calvert, S. E. and Price, N. B., *Contrib. Mineral. Petrol.*, 1970, **29**, 215–233.
5. Aller, R. C., *Adv. Geophys.*, 1980, **22**, 351–410.
6. Elderfield, H., Luedtke, N., McCaffrey, R. J. and Bender, M., *Am. J. Sci.*, 1981, **281**, 768–787.
7. Hunt, C. D., *Limnol. Oceanogr.*, 1983, **28**, 913–923.
8. Balzer, W., *Geochim. Cosmochim. Acta*, 1982, **46**, 1153–1161.
9. Sundby, B., Anderson, L. G., Hall, P. O. J., Iverfeldt, A., Rutgers, Van Der Loeff, M. M. and Westerland, S. F. G., *Geochim. Cosmochim. Acta*, 1986, **50**, 1281–1288.
10. Sayles, F. L., *Geochim. Cosmochim. Acta*, 1981, **45**, 1061–1086.
11. Emerson, S., Jahnke, R., Bender, M., Froelich, P., Klinkhammer, G., Bowser, C. and Setlock, G., *Earth Planet. Sci. Lett.*, 1980, **44**, 57–80.
12. Middleberg, J., Lange, G. J. and Weijden, C. H., *Geochim. Cosmochim. Acta*, 1987, **51**, 759–763.
13. Li, Y.-H., Bischoff, J. and Mathieu, G., *Earth Planet. Sci. Lett.*, 1969, **7**, 265–270.
14. Johnson, K. S., *Geochim. Cosmochim. Acta*, **46**, 1805–1809.
15. Aller, R. C., *Philos. Trans. R. Soc. London*, 1990, **A331**, 51–68.
16. Borole, D. V., Sarin, M. M., Somayajulu, B. L. K., *Indian J. Mar. Sci.*, 1982, **11**, 51–62.
17. Yadav, D. N., Sarin, M. M. and Somayajulu, B. L. K., in *Oceanography of the Indian Ocean* (ed. Desai, B. N.), Oxford & IBH, New Delhi, 1992, pp 359–367.
18. Somayajulu, B. L. K., Yadav, D. N. and Sarin, M. M., *Proc. Indian Acad. Sci. (Earth Planet. Sci.)*, 1994, **103**, 315–327.
19. Naqvi, S. W. A., Noronha, R. J., Somasundar, K. and Sengupta, R., *Deep-Sea Res.*, 1990, **37**, 593–611.
20. Lynn, D. C. and Bonatti, E., *Mar. Geol.*, 1965, **3**, 457–474.
21. Jones, C. J. and Murray, J. W., *Limnol. Oceanogr.*, 1985, **30**, 81–92.
22. Holdren, G. R. Jr., Bricker, O. P. III, and Matsoff, G., in *Marine Chemistry in the Coastal Environment*, (ed. Church, T. M.), A. C. S. Symposium Series no. 18, 1975, pp 364–381.
23. Klinkhammer, G. P. and Bender, M. L., *Earth Planet. Sci. Lett.*, 1980, **46**, 361–384.
24. Landing, W. M. and Bruland, K. W., *Earth Planet. Sci. Lett.*, 1980, **49**, 45–56.
25. Martin, J.H. and Knauer, G. A., *Earth Planet. Sci. Lett.*, 1980, **51**, 266–274.
26. Martin, J.H. and Knauer, G. A., *Earth Planet. Sci. Lett.*, 1984, **67**, 35–47.
27. Martin, J. M. and Meybeck, M., *Mar. Chem.*, 1979, **7**, 173–206.
28. Yadav, D. N., Unpublished Ph D thesis, M. S. University, Baroda, India, 1995, pp. 140.
29. Lyle, M. and Dymond, J. R., *Earth Planet. Sci. Lett.*, 1976, **30**, 164–168.
30. Saager, P. M., DeBaar, H. J. W. and Burkhill, P. H., *Geochim. Cosmochim. Acta*, 1989, **53**, 2259–2267.
31. Saager, P. M., *Proc. Indian Acad. Sci. (Earth Planet. Sci.)*, 1994, **103**, 237–278.
32. Johnson, K. S., Berelson, W. M., Coale, K. H., Coley, T. L., Elrod, V. A., Fairley, W. R., Lams, H. D., Kilgore, T. E. and Nowicki, J. L., *Science*, 1992, **257**, 1242–1245.
33. Sundby, B. and Silverberg, N., *Limnol. Oceanogr.*, 1985, **30**, 372–381.
34. Trefry, J. H. and Presley, B. J., *Geochim. Cosmochim. Acta.*, 1982, **46**, 1715–1726.
35. Yeats, P. A., Sundby, B. and Bowers, J. M., *Mar. Chem.*, 1979, **8**, 43–55.
36. Krishnaswami, S. and Lal, D., in *Lakes: Chemistry Geology Physics* (ed. Lerman, A.), Springer, New York, 1978, pp. 153–177.
37. DeMaster, D. J. and Cochran, J. K., *Earth Planet. Sci. Lett.*, 1982, **61**, 257–281.
38. Thamdrup, B., Fossing, H. and Jorgensen, B. B., *Geochim. Cosmochim. Acta*, 1994, **58**, 5115–5129.
39. Paropkari, A. L., Babuprakash, C. and Mascarenhas, A., *Mar. Geol.*, 1992, **107**, 213–226.
40. Heggie, D., Klinkhammer, G. and Cullen, D., *Geochim. Cosmochim. Acta*, 1987, **51**, 1059–1070.

ACKNOWLEDGEMENTS. Discussions with Profs S. Krishnaswami, B. L. K. Somayajulu and Dr M. M. Sarin were beneficial to the author during the course of this study. The critical reviews from Drs P. M. Saager and Tom Church greatly helped in improving the manuscript. Finally, I thank the Department of Ocean Development, New Delhi for generous help in funding the project.